

RESEARCH

Open Access



# Microglial dynamics after axotomy-induced retinal ganglion cell death

Francisco M. Nadal-Nicolás<sup>1,2,3\*</sup> , Manuel Jiménez-López<sup>1,2</sup>, Manuel Salinas-Navarro<sup>1,2</sup>, Paloma Sobrado-Calvo<sup>1,2</sup>, Manuel Vidal-Sanz<sup>1,2</sup> and Marta Agudo-Barriuso<sup>1,2\*</sup>

## Abstract

**Background:** Microglial cells (MCs) are the sentries of the central nervous system. In health, they are known as surveying MCs because they examine the tissue to maintain the homeostasis. In disease, they activate and, among other functions, become phagocytic to clean the cellular debris. In this work, we have studied the behavior of rat retinal MCs in two models of unilateral complete intraorbital optic nerve axotomy which elicit a different time course of retinal ganglion cell (RGC) loss.

**Methods:** Albino Sprague-Dawley rats were divided into these groups: (a) intact (no surgery), (b) fluorogold (FG) tracing from the superior colliculi, and (c) FG tracing + crush or transection of the left optic nerve. The retinas were dissected from 2 days to 2 months after the lesions ( $n = 4-12$  group/lesion and time point) and then were subjected to Brn3a and Iba1 double immunodetection. In each intact retina, the total number of Brn3a<sup>+</sup>RGCs and Iba<sup>+</sup>MCs was quantified. In each traced retina (b and c groups), FG-traced RGCs and phagocytic microglial cells (PMCs, FG<sup>+</sup>Iba<sup>+</sup>) were also quantified. Topographical distribution was assessed by neighbor maps.

**Results:** In intact retinas, surveying MCs are homogeneously distributed in the ganglion cell layer and the inner plexiform layer. Independently of the axotomy model, RGC death occurs in two phases, one quick and one protracted, and there is a lineal and topographical correlation between the appearance of PMCs and the loss of traced RGCs. Furthermore, the clearance of FG<sup>+</sup>RGCs by PMCs occurs 3 days after the actual loss of Brn3a expression that marks RGC death. In addition, almost 50% of MCs from the inner plexiform layer migrate to the ganglion cell layer during the quick phase of RGC loss, returning to the inner plexiform layer during the slow degeneration phase. Finally, in contrast to what happens in mice, in rats, there is no microglial phagocytosis in the contralateral uninjured retina.

**Conclusions:** Axotomy-induced RGC death occurs earlier than RGC clearance and there is an inverse correlation between RGC loss and PMC appearance, both numerically and topographically, suggesting that phagocytosis occurs as a direct response to RGC death rather than to axonal damage.

**Keywords:** Phagocyte, Iba1, Brn3a, Transcellular labeling, Migration, Fluorogold

## Background

In rodents, retinal ganglion cell (RGC) loss after optic nerve axotomy is a well-documented process that occurs in two phases [1]. The first one is quick and devastating, lasts around 14 days, and causes the loss of ~85% of RGCs. Then, RGC death takes a slower but steady pace

in such a way that 15 months after the injury, around 1% of the original population remains [2]. Furthermore, in rats, the rate of RGC loss is modulated by the distance from the optic nerve head at which the axotomy is performed, slower with longer distances [2, 3].

After axotomy, damaged RGCs die by apoptosis [4, 5]. Apoptotic cells initiate a highly controlled cascade of events that finishes when the cell bodies are cleared from the tissue by phagocytes [6, 7] which, in the central nervous system, are the microglial cells (MCs).

\* Correspondence: fm.nadalnicolas@um.es; martabar@um.es

<sup>1</sup>Grupo de Oftalmología Experimental, Instituto Murciano de Investigación Biosanitaria-Virgen de la Arrixaca, Edificio LAIB Planta 5ª, Carretera Buenavista s/n, 30120 El Palmar, Murcia, Spain

Full list of author information is available at the end of the article

In the healthy retina, MCs are located on four layers: the retinal nerve fiber layer (RNFL) that contains RGC axons; the ganglion cell layer (GCL), where RGC somata and displaced amacrine cells lie; the inner plexiform layer (IPL); and the outer plexiform layer (OPL). While plexiform layers are mainly formed by neuropil, the IPL also contains displaced RGCs (dRGCs) [8].

MC surveys the tissue (surveying MCs (SMCs)), keep the homeostasis, and stabilize the synapses [9, 10]. Upon neuronal death, MCs activate [11, 12] and migrate to the damaged region [13] to participate in the careful clearance of cellular debris and to repair the local damage (reviewed in [14–16]). This removal is critical to maintain tissue integrity (reviewed in [17]).

The phagocytic uptake of MCs can be measured *in vitro* by different assays such as administration of fluorescent bioparticles or cell debris previously labeled [18]. *In vivo*, phagocytic microglial cells (PMCs) can be identified by transcellular labeling, a process that occurs when a MC engulfs a dying fluorescent neuron [19–24]. This is a powerful approach to study PMC behavior and tissue clearing, provided that a given neuronal population is first labeled and then injured.

In rats and mice, almost the whole population of RGCs (~98% [25, 26]) can be traced from both superior colliculi with fluorogold (FG), a fluorescent retrograde tracer. Thus, if after RGC tracing the optic nerve is injured, it is possible to assess at the same time RGC clearance and the appearance of transcellularly labeled MCs [21–24]. Using this tool in mice, we have shown that after unilateral axotomy, the appearance of PMCs and the clearance of traced RGCs in the injured retina are linearly correlated [21, 24]. Interestingly, in the contralateral uninjured retina of pigmented mice, some MCs become phagocytic and their number and distribution are constant and independent of RGC survival in the injured retina.

There are many works describing the microglial response to injury, activation mechanisms and phenotypes, and release of inflammatory mediators or their involvement in neurodegeneration and neuroprotection [27–33]. But little is known of their numerical and topographical dynamics and their correlation with the dying neurons, for instance, is the temporal and topographical course of PMC appearance regulated by the course of neuronal death? Is neuronal clearance the same as neuronal death? Is there a contralateral retinal response involving PMC appearance in adult rats? Do MCs travel from the outer retinal layers to the inner retina to cope with the massive RGC death triggered by axotomy?

To answer these questions, we have used RGC tracing and immunodetection of microglial cells (Iba1) and

viable RGCs (Brn3a) in the same retinas after two different axotomy models.

## Methods

### Animal handling

Adult female albino Sprague-Dawley rats (200 g,  $n = 80$ ) were obtained from the University of Murcia breeding colony. All animals were treated in compliance with the European Union guidelines for Animal Care and Use for Scientific Purpose (Directive 2010/63/EU) and the guidelines from the Association for Research in Vision and Ophthalmology (ARVO) Statement for the Use of Animals in Ophthalmic and Vision Research. All procedures were approved by the Ethical and Animal Studies Committee of the University of Murcia, Spain (REGA 300305440012).

Animals undergoing surgery were anesthetized by intraperitoneal injection of a mixture of ketamine (60 mg/kg; Ketolar, Pfizer, Alcobendas, Madrid, Spain) and xylazine (10 mg/kg; Rompum, Bayer, Kiel, Germany). Analgesia was provided by subcutaneous administration of buprenorphine (0.1 mg/kg; Buprex, buprenorphine 0.3 mg/mL; Schering-Plough, Madrid, Spain). During and after surgery, the eyes were covered with an ointment (Tobrex; Alcon, S. A., Barcelona, Spain) to prevent corneal desiccation.

The animal groups are the following: (i) intact, no surgery; (ii) tracing controls, tracing from the superior colliculi (SCi), analyzed 7 days or 2 months later (9 weeks); (iii) axotomized, tracing from the SCi, and 1 week later optic nerve crush (ONC) or optic nerve transection (ONT), retinal analysis 2, 5, 9, 14 days or 2 months (9 weeks tracing) later. Injured retinas are the left ones, and contralateral retinas the right ones.

### Retrograde tracing

After the exposure of both SCi, a pledge of gelatin sponge soaked in 3% fluorogold (FG, Fluorochrome, LLC, USA) dissolved in 10% dimethyl sulfoxide/saline was applied onto both SCi 7 days prior optic nerve injury, or 7 days or 9 weeks before sacrifice (traced but otherwise intact retinas), following standard techniques in our laboratory [8, 23, 24, 34, 35].

### Optic nerve injuries

Seven days after RGC tracing and according to previous studies, the left optic nerve was crushed or transected at 3 or 0.5 mm from the optic disc, respectively [2, 4, 34–36]. With these settings, ONC elicits a slower RGC death than ONT [2, 34].

### Tissue preparation and sectioning

Unless otherwise stated, all reagents were from Sigma-Aldrich Quimica S.A. Madrid, Spain.

Animals were sacrificed with an intraperitoneal injection of an overdose of sodium pentobarbital (Dolethal, Vetoquinol; Especialidades Veterinarias, S.A., Alcobendas, Madrid, Spain). All animals were perfused transcardially with 0.9% saline solution followed by 4% paraformaldehyde in 0.1 M phosphate buffer.

The retinas ( $n = 4\text{--}12$ /group and time point, see tables) were dissected as flattened whole mounts as previously described [34]. Some eye cups ( $n = 3$ /group and time point) were cryoprotected in a series of sucrose gradients, embedded in optimal cutting temperature medium (OCT, Tissue-Tek, Sakura-Finetek, VWR, Barcelona, Spain), frozen, and sectioned in a cryostat at 14- $\mu\text{m}$  thickness.

### Immunohistofluorescence

Double immunodetection of RGCs and MCs was carried out as previously described [2, 11, 21, 35, 37]. Healthy RGCs were detected using goat  $\alpha$ -Brn3a (C-20; Santa-Cruz Biotechnology, Heidelberg, Germany) diluted 1:750 and microglial cells using rabbit  $\alpha$ -Iba1 antibody (ionized calcium-binding adapter molecule 1; Wako Chemicals GmbH, Neuss, Germany) diluted 1:1000. Secondary detection was carried out with donkey  $\alpha$ -goat and donkey  $\alpha$ -rabbit (Alexa Fluor 594 and 488 respectively; Molecular Probes; Thermo Fisher Scientific, Madrid, Spain) diluted at 1:500. In some retinal sections, all nuclei were counterstained using antifading mounting media with DAPI (4',6-diamidino-2-phenylindole, Vectashield mounting medium with DAPI; Vector Laboratories, Palex Medical, Barcelona, Spain).

### Image acquisition

Whole-mounted retinas were photographed focusing firstly on the GCL and secondly on the IPL. All images were acquired using an epifluorescence microscope (Axioscop 2 Plus; Zeiss Mikroskopie, Jena, Germany) equipped with a computer-driven motorized stage (ProScan H128 Series; Prior Scientific Instruments, Cambridge, UK) controlled by image analysis software (Image-Pro Plus, IPP 5.1 for Windows; Media Cybernetics, Silver Spring, MD). Retinal photomontages were reconstructed from 154 ( $11 \times 14$ ) individual images by zigzag tiling, as reported [2, 25, 38].

### Quantification

FG<sup>+</sup>RGCs in intact and contralateral to the lesion retinas, and Brn3a<sup>+</sup>RGCs in all retinas, were automatically quantified using our previously described methods [25, 34]. After injury, microglial cells became transcellularly labeled (PMCs: FG<sup>+</sup>Iba1<sup>+</sup>), being for the automated routine impossible to tell them apart from traced RGCs. Thus, FG<sup>+</sup>RGCs were manually quantified (FG<sup>+</sup>Iba1<sup>-</sup>) and their total number estimated using previously

reported methods [11]. Briefly, the retinas were divided into three concentric rings (central, equatorial, and peripheral) and four samples within each were selected (0.25 mm<sup>2</sup>/sample). Each sample corresponded to a retinal quadrant, therefore, three samples per quadrant and four samples per ring. The area of each ring was measured, and the total number of FG<sup>+</sup>RGCs in a given ring were estimated from the mean number quantified in its four samples, thus giving back the number of FG<sup>+</sup>RGCs in the central, medial, and peripheral retina. The total number of FG<sup>+</sup>RGCs per retina was the sum of the partial values. This method was validated in intact retinas, where FG<sup>+</sup>RGCs were quantified automatically and manually (for more details, see [11]).

All non-phagocytic MCs (Iba1<sup>+</sup>FG<sup>-</sup>) and PMCs (Iba1<sup>+</sup>FG<sup>+</sup>) were manually dotted on the retinal photomontages using Adobe Photoshop CS 8.0.1; (Adobe Systems, Inc., San Jose, CA), and the dots were automatically quantified (IPP software) [2, 8, 24, 39]. Quantitative data from all populations were exported to a spreadsheet application (Microsoft Office Excel 2003; Microsoft Corporation, Redmond, WA) for further analyses.

### Spatial distribution

The spatial distribution of RGCs and MCs was assessed by the near neighbor algorithm as reported [2, 21, 24, 39, 40]. The position of each Brn3a<sup>+</sup>RGC or dot (microglial cell) in the photomontage was translated to an  $X,Y$  location using as reference the optic nerve (0,0 point). Maps were plotted using SigmaPlot (SigmaPlot 9.0 for Windows; Systat Software, Inc., Richmond, CA, USA). In addition, using a color code, these maps depict the number of neighbors around a given cell in a given radius (see Fig. 1 legend).

### Statistical analysis

Data were analyzed with GraphPad Prism v.7 (GraphPad San Diego, USA). Each cell type was analyzed independently along time within each lesion and between lesions (one-way ANOVA, post hoc Tukey's test). Differences were considered significant when  $p < 0.05$ . Data are presented as mean  $\pm$  standard deviation. Correlation analyses (microglial cells vs. RGCs, or cells vs. time) were modeled using the same program and were considered significant when  $R^2$  (goodness of the fit) was  $\geq 0.9$ .

### Results

In all the retinas except the intact ones, RGCs were identified by Brn3a immunodetection and tracing. The loss of Brn3a signal announces that a RGC is dead [2, 4]. A traced RGC might not be viable (no Brn3a expression), but it may still be detectable because the FG filling the RGC soma is an exogenous compound that will disappear from the tissue only upon microglial clearance.

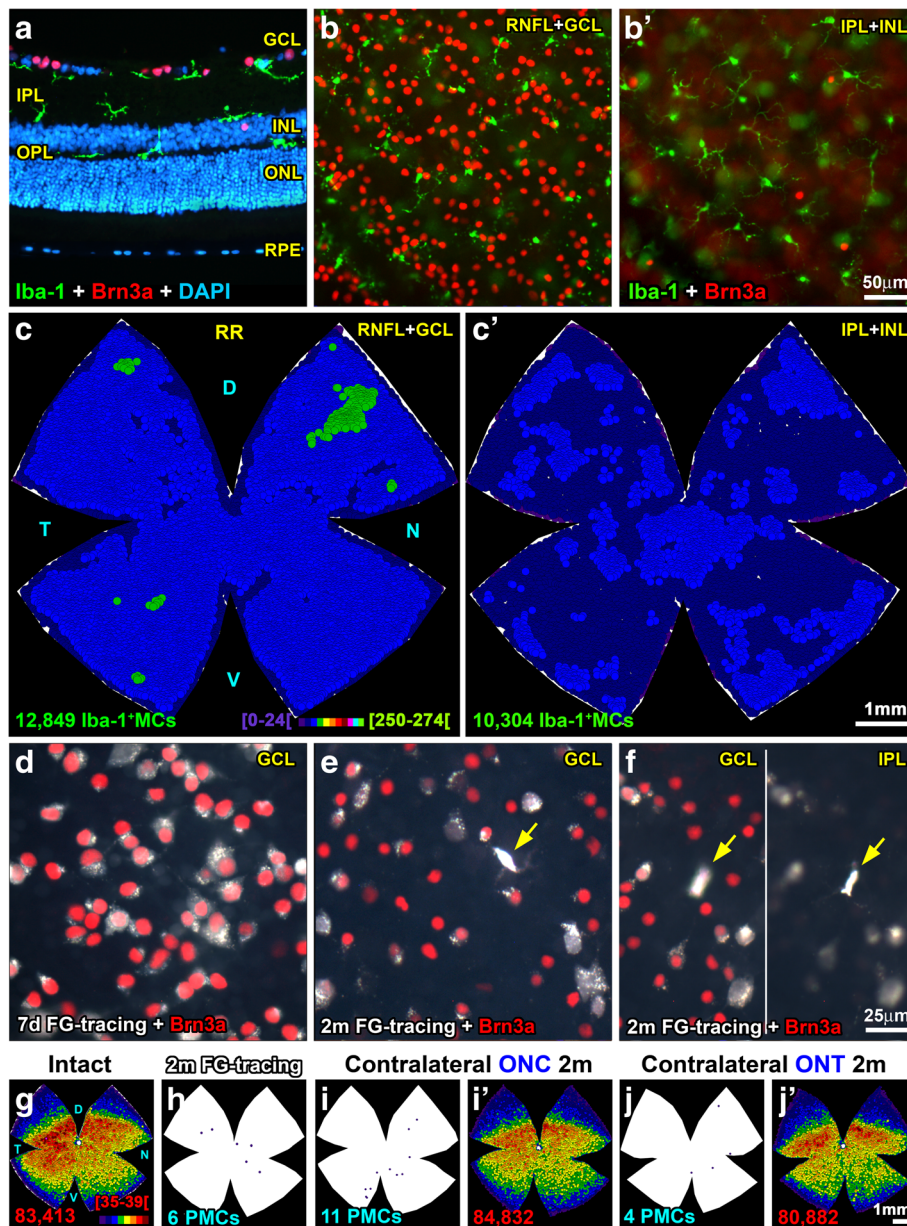


**Fig. 1** Microglial cells are homogeneously distributed in intact retinas. **a** Cross section showing the location of Iba1<sup>+</sup>MCs (green) and Brn3a<sup>+</sup>RGCs (red) in intact retinas. Note that some MCs in the IPL are lying on top of the INL. **b** Magnification from an intact flat-mounted retina focused on the RNFL/GCL showing Iba1<sup>+</sup>MCs and Brn3a<sup>+</sup>RGCs. **b'** Iba1<sup>+</sup>MCs and displaced Brn3a<sup>+</sup>RGCs in the same area as **b** but changing the focus to the IPL/INL. **c** Neighbor map of an intact retina showing the distribution of MCs in the GCL. **c'** Neighbor map from the same retina showing the distribution of MCs in the IPL. **d** Magnification from a control retina 7 days after fluorogold tracing (white), immunodetected with Brn3a (red). In these retinas, no PMCs were observed. In control retinas analyzed 2 months after tracing (**e, f**) some PMCs (yellow arrows) were observed in the GCL (**e, f** left) and IPL (**f** right). **g** Neighbor map of an intact retina showing the distribution of Brn3a<sup>+</sup>RGCs. **h** Retinal outline showing the position of the few PMCs found in control retinas analyzed 2 months after tracing. **i, j** Retinal outlines showing the location of the PMCs found in contralateral to the lesion retinas analyzed 2 months after the unilateral ONC (**i**) or ONT (**j**). **i', j'** Brn3a<sup>+</sup>RGCs neighbor maps from the same retinas as in **i, j**. For this and the subsequent figures: The number of cells represented is shown below each map. Neighbor maps represent the number of neighbors around each cell (dot) within a given radius and color scale. For MC representation, the radius is 0.276 mm and the scale (**c**, bottom) goes from 0 to 24 (purple) to ≥ 250–274 neighbors (bright green). For RGCs, the radius is 0.0552 mm and the color scale (**g**, bottom) goes from 0 to 4 (purple) to ≥ 35–39 (dark red) neighbors. D dorsal, V ventral, T temporal, N nasal, RR right retina, RNFL retinal nerve fiber layer, GCL ganglion cell layer, IPL inner plexiform layer, INL inner nuclear layer, OPL outer plexiform layer, ONL outer nuclear layer, ONC optic nerve crush, ONT optic nerve transection, MC microglial cell, PMC phagocytic microglial cell, m months, d days

In intact retinas, MCs are called surveying MCs (Iba1<sup>+</sup>). In the experimental retinas, we counted Iba1<sup>+</sup>FG<sup>+</sup> PMCs, and Iba1<sup>+</sup>FG<sup>-</sup> MCs that may or may not have been activated, for accuracy, and we termed them non-phagocytic microglial cells (non-PMCs).

We could not discriminate between the RNFL and GCL. Also, we acquired images from the IPL and the inner limit of the inner nuclear layer (INL) because we used the dRGCs as pegs. For simplicity, we will refer to these layers in the text as GCL or IPL, respectively.

### Intact retinas

As observed in the retinal section in Fig. 1a, SMCs are found in the GCL, IPL, and OPL. In the IPL, some MCs lie on the inner limit of the INL. Using flat mounts, we quantified their total number in the GCL or IPL (Fig. 1b, b'), which contain, respectively, RGC axons and somata, or their dendrites and dRGCs.

The total number of SMCs in the GCL and IPL is very similar (Table 1), although slightly higher in the GCL. The ratio RGC/MC is 6:1 if we take into account only MCs in the GCL, but if we add the MCs in the IPL, that is MCs in the GC complex, this ratio becomes 3:1. In both layers, SMCs are homogeneously distributed (Fig. 1c, c'; Table 1).

### Tracing controls and contralateral retinas

In traced retinas, FG is observed filling the RGC cytoplasm, while Brn3a expression is nuclear (Fig. 1e). When the tracer is left for 7 days (standard procedure), there are usually no visible PMCs (Table 1). By 2 months, few PMCs are observed, both in the GCL and IPL. Note that at 2 months, the number of FG<sup>+</sup>RGCs decreases

because FG is not a persistent label [39, 41, 42] but the number of Brn3a<sup>+</sup>RGCs remains unaltered (Fig. 1f–i, Table 1). In the right retinas, contralateral to the lesion, there is no RGC loss and the presence of PMCs is testimonial (Fig. 1i, j'; Table 1).

### RGC death vs. RGC clearance

After ONC or ONT, traced RGCs disappear and PMCs appear (Fig. 2a–j). The morphology of MCs after the lesion changes from ramified to fusiform or ameboid. Fusiform or rod-like MCs are preferentially found in chains, along the RGC axons. Ameboid MCs are found more often engulfing a traced RGC which, normally, does not express Brn3a anymore (Figs. 2 and 3a).

As previously reported [2, 34], RGC loss after ONC is slower than after ONT, and this is observed with both identification methods (Table 2 and Fig. 3b, c). However, there are differences between the course of RGC death (Brn3a) and RGC clearance (FG).

Within each lesion, RGC loss is detected earlier with Brn3a than with FG. Indeed, half of the RGCs have died 5.6 days after ONC or 4.2 days after ONT, while half of the RGC clearance occurs 3 days later for both lesions (at 7.2 or 8.4 days respectively). Furthermore, RGC death adjusts to a segmental lineal regression with two phases of loss, one quick that lasts up to 7 days for ONC (daily loss of 7326 RGCs,  $m_1$ ) or to 5.8 days for ONT ( $m_1$ , 9762 RGCs/day) and a slower one thereafter with a comparable rate of loss for both lesions ( $m_2$  values). For its part, RGC clearance is linear and the daily disappearance rate is similar between lesions (there are no significant differences in the slopes between ONC and ONT

**Table 1** Intact, tracing control, and contralateral to the injury retinas

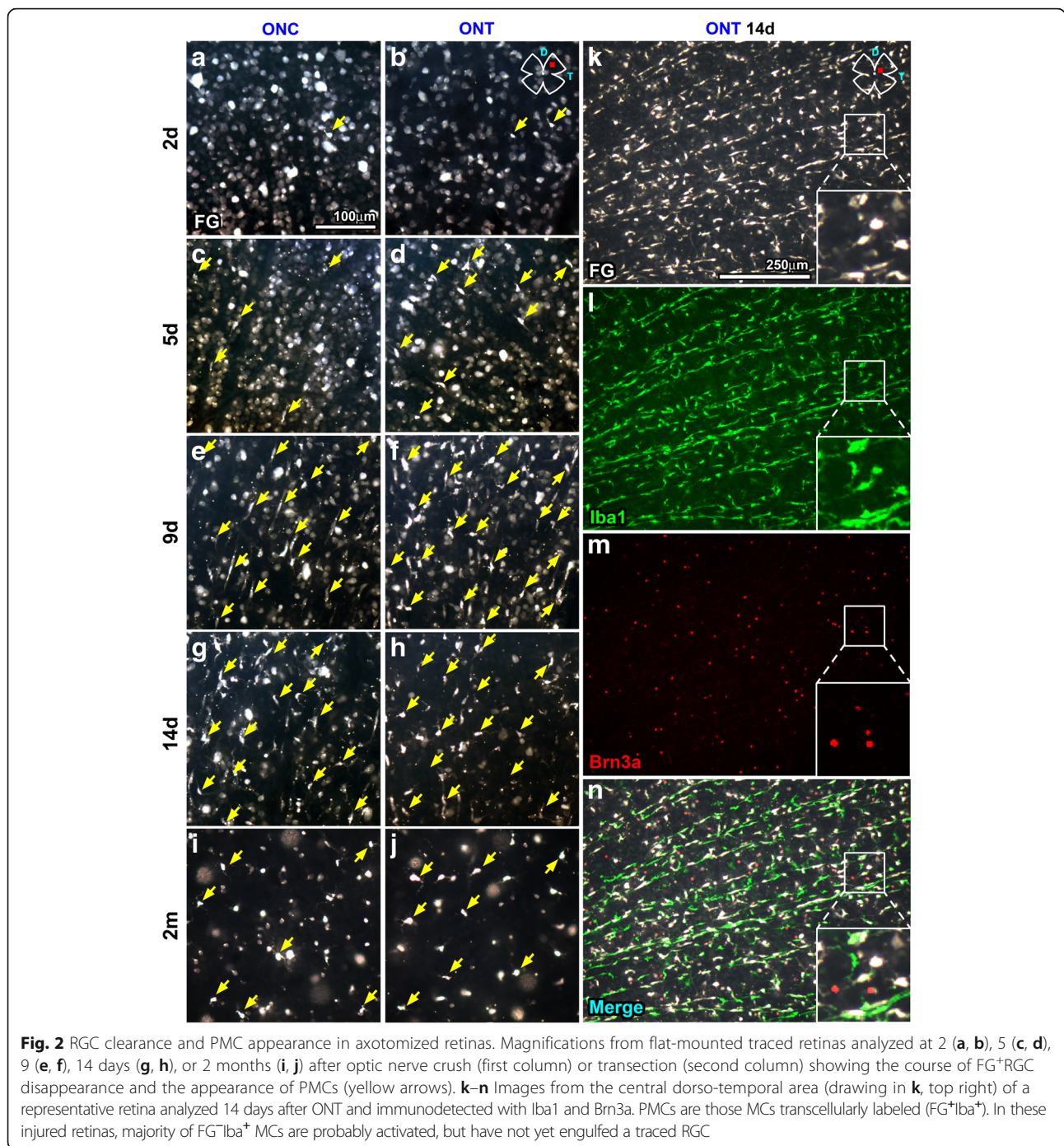
		Intact (n = 4)	Tracing control		Contralateral (n = 80/72*)
			7 days (n = 8)	2 months (n = 4)	
RNFL/GCL	Brn3a <sup>+</sup> RGCs	82,530 ± 766	81,504 ± 798	81,368 ± 491	81,486 ± 2272
	FG <sup>+</sup> RGCs		81,829 ± 1246	58,948 <sup>§</sup> ± 3381	81,513 ± 1425
RNFL/GCL	SMCs	14,151 ± 1186			
	PMCs		0 ± 0	6 ± 2	1 ± 3
IPL/INL	SMCs	11,006 ± 989			
	PMCs		0 ± 0	1 ± 1	
GCC	SMCs	25,156 ± 1367	0 ± 0		
	PMCs		0 ± 0	7 ± 3	

Mean number ± standard deviation of Brn3a<sup>+</sup>RGCs, FG<sup>+</sup>RGCs, surveying microglial cells (SMCs), and phagocytic microglial cells (PMCs) counted in the same retinas within each group. PMCs were quantified in the retinas that had been traced with fluorogold 7 days or 2 months before sacrifice to match the tracing standard (7 days) and the longer tracing times used in the injured retinas (see Table 2)

FG fluorogold, RGCs retinal ganglion cells, RNFL/GCL retinal nerve fiber layer/ganglion cell layer, IPL/INL inner plexiform layer + inner limit inner nuclear layer, GCC ganglion cell complex (RNFL/GCL + IPL/INL)

<sup>§</sup>The number of FG<sup>+</sup>RGCs 2 months after tracing is significantly smaller than at 7 days because FG is not a permanent dye [39, 41, 42], while the number of Brn3a<sup>+</sup>RGCs remains unaltered. In 2-month traced retinas, there are some PMCs, although this is not significant compared to 7 days of tracing or intact retinas (one-way ANOVA, Tukey's post hoc test,  $p > 0.05$ )

\*The number of contralateral retinas amounts to 80 for Brn3a<sup>+</sup>RGCs and PMCs (see Table 2) and to 72 for FG<sup>+</sup>RGCs (2-month time point excluded). No significant differences were observed between contralateral and control or intact retinas (one-way ANOVA test, Tukey's post hoc test,  $p > 0.05$ )



$p = 0.59$ ), albeit delayed for 1 day (see above) and less pronounced after ONC (5249 RGCs/day) than after ONT (5795 RGCs/day).

### PMC dynamics

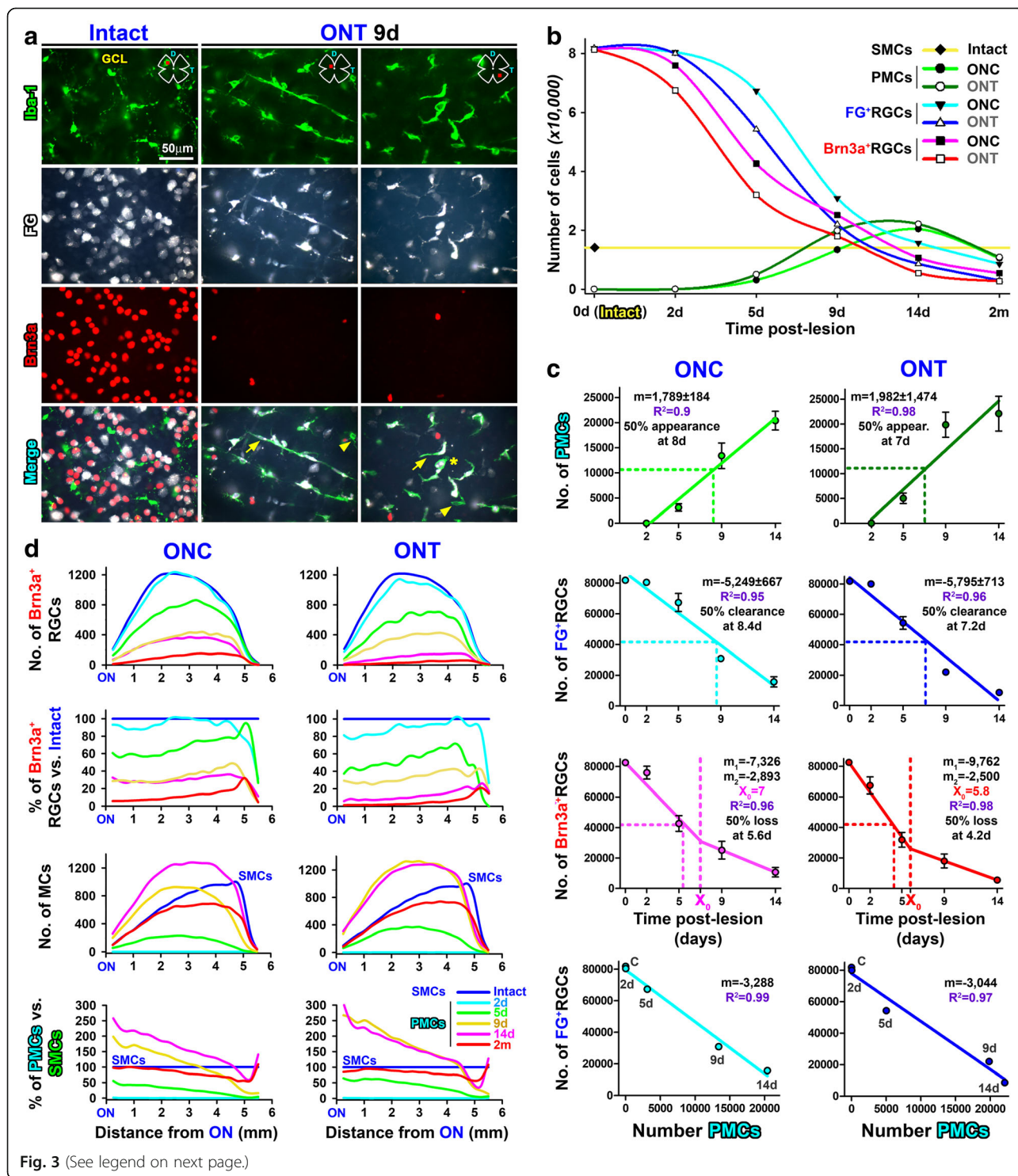
PMC appearance highly correlates with FG clearance (Fig. 3c), but not as much with RGC death (Brn3a<sup>+</sup>RGCs vs. PMCs, regression coefficient 0.84, not shown). Incidentally, the FG<sup>+</sup>RGCs vs. PMCs

correlation tells us that for each 3288 or 3044 cleared RGCs, there is an increase of 1000 PMCs, meaning that one PMC is able to engulf ~3 RGCs. This ratio can also be estimated from the slope of FG<sup>+</sup>RGCs vs. time by the slope of PMCs vs. time (i.e.,  $5249/1789 = 2.9$ ).

Quantitative analyses of cell topography show that more RGCs die in the central retina (Fig. 3d, first graph). Proportionately, though, their death is synchronous

along the retina because the percent of loss is similar at any given distance from the optic nerve (Fig. 3d, second graph). In agreement, PMCs appear across the GCL, increasing in number with increasing post-lesion intervals, following the topographic pattern of RGC loss (Fig. 3d, compare the third graph with the first one). However,

proportionally, the central retina bears a higher percent of PMCs than the periphery (Fig. 3d, fourth graph). This can be explained because there are more PMCs where more RGCs are dying, and this is clearly observed when the data are graphed as neighbor maps (Fig. 4); while RGC loss is diffuse, the



(See figure on previous page.)

**Fig. 3** Microglial cell morphologies, quantitative topography, and correlation analyses of PMC appearance, RGC clearance, and RGC death. **a** Microglial cells in control or axotomized retinas: magnifications from control or injured FG-traced retinas immunodetected for Iba1 and Brn3a taken from the red areas shown in the retinal drawing. Arrows, PMCs. Arrowheads, activated MCs that have not yet engulfed a traced RGC. Asterisk, MC engulfing a traced RGC that has lost its Brn3a expression. **b** Temporal course of RGC loss and PMC appearance. The yellow line is the number of SMCs in intact retinas. **c** Correlation analyses created from total mean numbers  $\pm$  standard deviation. First row, PMCs vs. time; lineal fit. Second row, FG<sup>+</sup>RGCs vs. time; lineal fit. Third row, Brn3a<sup>+</sup>RGCs vs. time; lineal segmental fit. Fourth row, FG<sup>+</sup>RGCs vs. PMCs; lineal fit.  $R^2$  is the correlation coefficient.  $m$  is the slope of the straight line.  $X_0$  is the day when the first linear phase of RGC loss changes to a second, slower one.  $m_1$  and  $m_2$  are the slopes of the first and second linear phases, respectively. Fifty percent appearance, clearance, or loss is the time (days) when, according to the mathematical analysis, half of the PMCs have appeared, half of the RGCs have been cleared from the tissue, or half of the RGCs have died, respectively. Left column ONC, right column ONT. **d** Quantitative topography. Line graphs where the mean number or percent of cells (Y-axis) counted after ONC (left column) or ONT (right columns) are plotted against the length of the retina (X-axis) being 0 the optic nerve and 6 mm the periphery. First row, number of Brn3a<sup>+</sup>RGCs. Second row, Brn3a<sup>+</sup>RGCs as percent of intact retinas (blue line). Third row, number of MCs, which are surveying MCs for intact retinas and PMCs for injured ones. Fourth row, percent of PMCs, being 100% the number of SMCs in intact retinas (blue line)

emergence of PMCs seems centripetal being their density higher in the retinal areas where RGCs are more abundant (RGC distribution in an intact retina, Fig. 1g).

#### Microglial migration between layers

PMCs peak at 14 days (Table 2). At this time point, ~90% of MCs in the GCL are PMCs which, as abovementioned, are more abundant in the areas of higher RGC density and death (Fig. 5a, e). The remaining 10% are non-PMCs and are distributed fairly homogeneously, except for a dense accumulation around the optic nerve and along the extreme periphery (Fig. 5a', e').

At its highest, the number of PMCs + non-PMCs in the GCL surpasses the number of SMCs found in intact retinas by ~10,000. In parallel, there is a uniform decrease of MCs in the IPL (around 50% of their initial population) that justifies half of the excess observed in the GCL, suggesting that there is microglial migration between these layers (Table 2, Fig. 5b–b", f–f"). Indeed, PMCs are observed orthogonally placed in the IPL and INL from 9 days onwards (Fig. 6).

Two months after the lesions, when RGC death has slowed down, the number of MCs in the GCL has decreased and is numerically (Table 2) and topographically (Fig. 5c–c", g–g") normal, albeit most of these MCs are still transcellularly labeled. For its part, the IPL has partially recovered by the addition of PMCs which, most probably, come from the GCL (Table 2, Fig. 5d–d", h–h"). However, the IPL, and therefore the GC complex, are deficient on 3000–5000 MCs compared to that on intact retinas.

#### Discussion

We describe here for the first time the numerical, mathematical, and topographical relationship between RGCs and MCs in healthy and injured rat retinas. The strengths of this work lie firstly on the fact that RGCs are the only retinal neurons that die after optic nerve axotomy [2, 43–45] and, secondly, on the analysis of whole populations in the same retinas, using markers of

RGC viability and clearance in combination with the identification of phagocytic and non-phagocytic microglial cells. We have limited our study to the retinal layers where the RGC axons, somata, and processes are and focused the analysis on the phagocytic response rather than on microglial activation [46–49].

#### Intact retinas

In agreement with previous reports, MCs are homogeneously distributed in the GCL and IPL of healthy retinas [46, 49]. This topography reflects their surveying function, explained by the continuous mobility of MCs and their multidirectional projections used to maintain the distance between surrounding cells [50].

In traced but otherwise intact rat retinas, the number of PMCs depends on the time of tracing, as it has been shown in mice [21]. In these retinas, we did not observe a significant loss of Brn3a<sup>+</sup>RGCs (at least up to 2 months). Thus, the presence of PMCs can be explained by phagocytosis of the FG excreted by the traced RGCs, by pruning of RGC neurites, and/or by direct toxicity of the tracer on a few RGCs. Our study does not allow to discriminate among these reasons, but given the very low number of PMCs quantified in these control retinas, tracing itself does not influence PMC quantification after injury.

#### Contralateral uninjured retinas

In mice, after unilateral ON axotomy, there is a strong PMC reaction in the contralateral (uninjured) retina that is constant, scattered, and independent of the rate of RGC survival in the axotomized retina [21, 24]. In rats, a contralateral response involving activation of MCs, astrocytes, and Müller cells has been observed after axotomy [47, 51–54], or ocular hypertension [55], but to our knowledge, this is the first report describing that in this species, there is not a PMC reaction. At present, we do not know why, but it is possible that the scarce retino-retinal projection is implicated because in adult rats, this projection is missing in some animals and, when present, is smaller than in mice [56–58]. Thus, retino-retinal RGCs, which are directly

**Table 2** Injured retinas

	Retinal nerve fiber layer/ganglion cell layer				Inner plexiform layer			Ganglion cell complex (GCL + IPL)
	Bm3a <sup>+</sup> RGCs	FG <sup>+</sup> RGCs	PMCs	Non-PMCs	PMCs	Non-PMCs	Total MCs	
ONC								
2 days (n = 8)	75,987 ± 4210	80,459 ± 1552	11 ± 5					
5 days (n = 8)	42,656* ± 5111	67,302* ± 5901	3116* ± 740					
9 days (n = 8)	25,105* ± 5789	30,896* ± 1719	13,401* ± 2549					
14 days (n = 12)	10,639* ± 3150	15,755* ± 3359	22,404* ± 1863	2801 ± 350	760* ± 132	4501 ± 546	<b>5261* ± 404</b>	<b>28,467 ± 1555</b>
2 months (n = 4)	5457 ± 1724	8580* ± 385	10,497* ± 289	2375 ± 408	2343 ± 304	4694 ± 499	<b>7038* ± 660</b>	<b>19,910* ± 948</b>
ONT								
2 days (n = 8)	67,466*† ± 5539	79,997 ± 1345	43 ± 8					
5 days (n = 8)	31,938*† ± 4829	54,290*† ± 4136	5025* ± 1058					
9 days (n = 8)	18,015* ± 4542	22,002*† ± 1336	19,842*† ± 2534					
14 days (n = 12)	5515* ± 1101	8627*† ± 1433	22,092† ± 3514	2258 ± 412	941* ± 211	4760 ± 801	<b>5702* ± 792</b>	<b>30,053 ± 2202</b>
2 months (n = 4)	2708 ± 813	2983* ± 232	10,865* ± 584	3280 ± 685	3971† ± 125	3756 ± 356	<b>7728* ± 332</b>	<b>21,873* ± 415</b>

Mean number ± standard deviation of Bm3a<sup>+</sup>RGCs, FG<sup>+</sup>RGCs, phagocytic microglial cells (PMCs), and non-phagocytic microglial cells (non-PMCs, surveying and/or activated microglial cells that are not transcellularly labeled) in the same retinas within each group and time point. Total MCs is the sum of PMCs and non-PMCs

MC microglial cell, FG fluorogold, RGCs retinal ganglion cells, ONT optic nerve transection, ONC optic nerve crush, RNFL/GCL retinal nerve fiber layer + ganglion cell layer, IPL/INL inner plexiform layer + inner limit inner nuclear layer, GCC ganglion cell complex (RNFL/GCL + IPL/INL)

\*Significant difference compared to previous time point (2 days or IPL 14 days vs. intact or tracing control retinas, Table 1)

†Significant difference between ONC and ONT at the same time point. One-way ANOVA and Tukey's post hoc test, *p* < 0.05. The number of analyzed retinas to quantify GCL cells is shown in the second left column. For the IPL analysis, four retinas per group/time point were used

In bold font is shown the total number ± SD of MCs (PMCs plus non-PMCs) in the different retinal layers

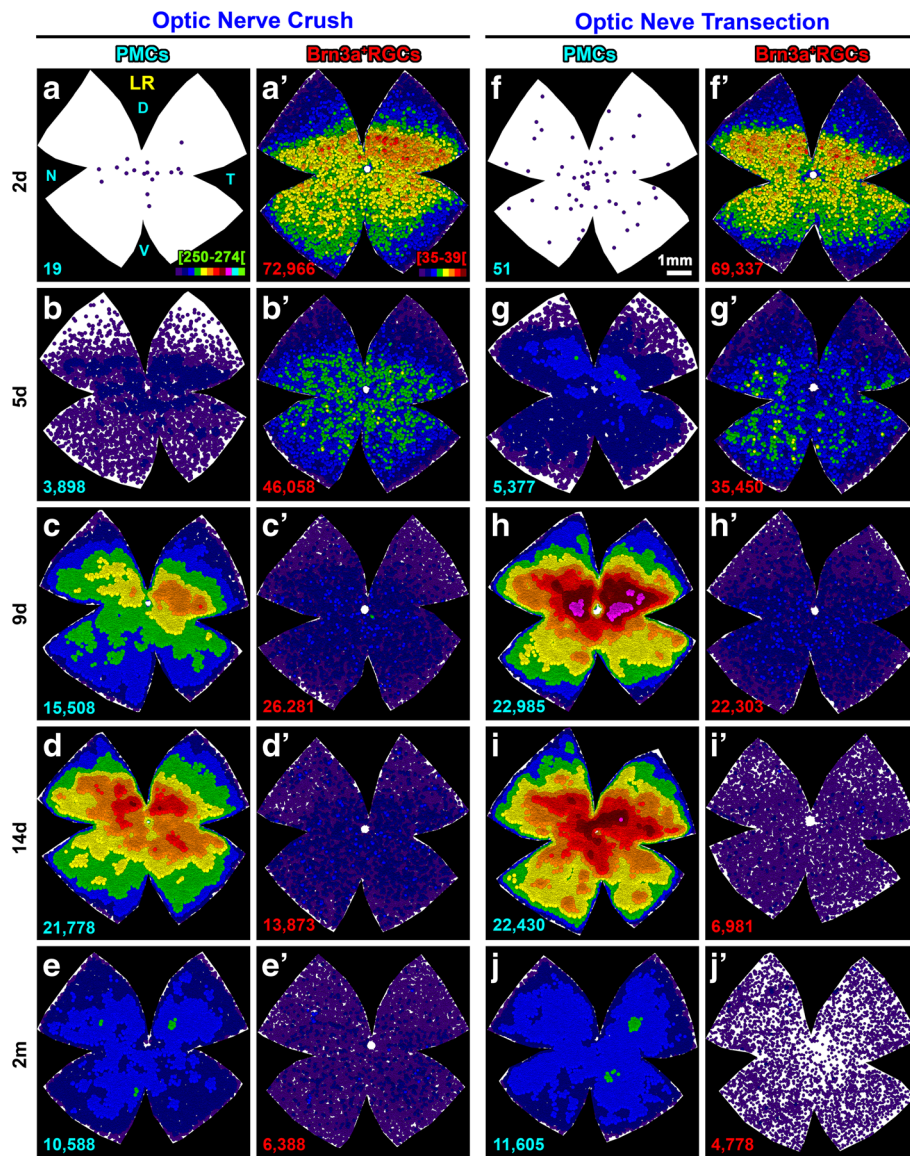


**Fig. 4** Topographic correlation of PMC appearance and RGC death. Neighbor maps showing the spatial distribution of PMCs (a–j) and Brn3a<sup>+</sup>RGCs (a’–j’) in the same retinas within each group and time point after optic nerve transection (a–e’) or crush (f–j’). Map description is in Fig. 1 legend

affected by the axotomy, could transmit a danger signal that would spread along the retina, recruiting and activating MCs. These signals would not be sufficient to elicit a PMC response in those rats with very few retino-retinal RGCs, and inexistent in those animals without them. In addition, these signals might combine with a systemic inflammatory response that would account for the inflammatory reaction observed in both species.

#### Microglial morphology

The role of MCs in neurodegenerative diseases is controversial, but it is clear that they are not simple bystanders [27]. For one part, MCs restore tissue homeostasis,

keeping the neuronal interactions as healthy as possible [9, 10], and their suppression improves axonal regeneration and RGC survival after axotomy [59]. On the other hand, MC over-activation may be damaging [31], as they act as mediators of the inflammatory response observed in several retinal degenerative diseases (reviewed in [60]), although in this respect there is some debate [61].

Upon neuronal death, MCs change their morphology from a surveying ramified shape to an ameboid-like one, M1 phenotype, which is considered harmful [28, 62–65]. Here, we show that ameboid PMCs are often found engulfing RGC somas. We also found phagocytic rod-shaped MCs, especially along the intraretinal axons, in

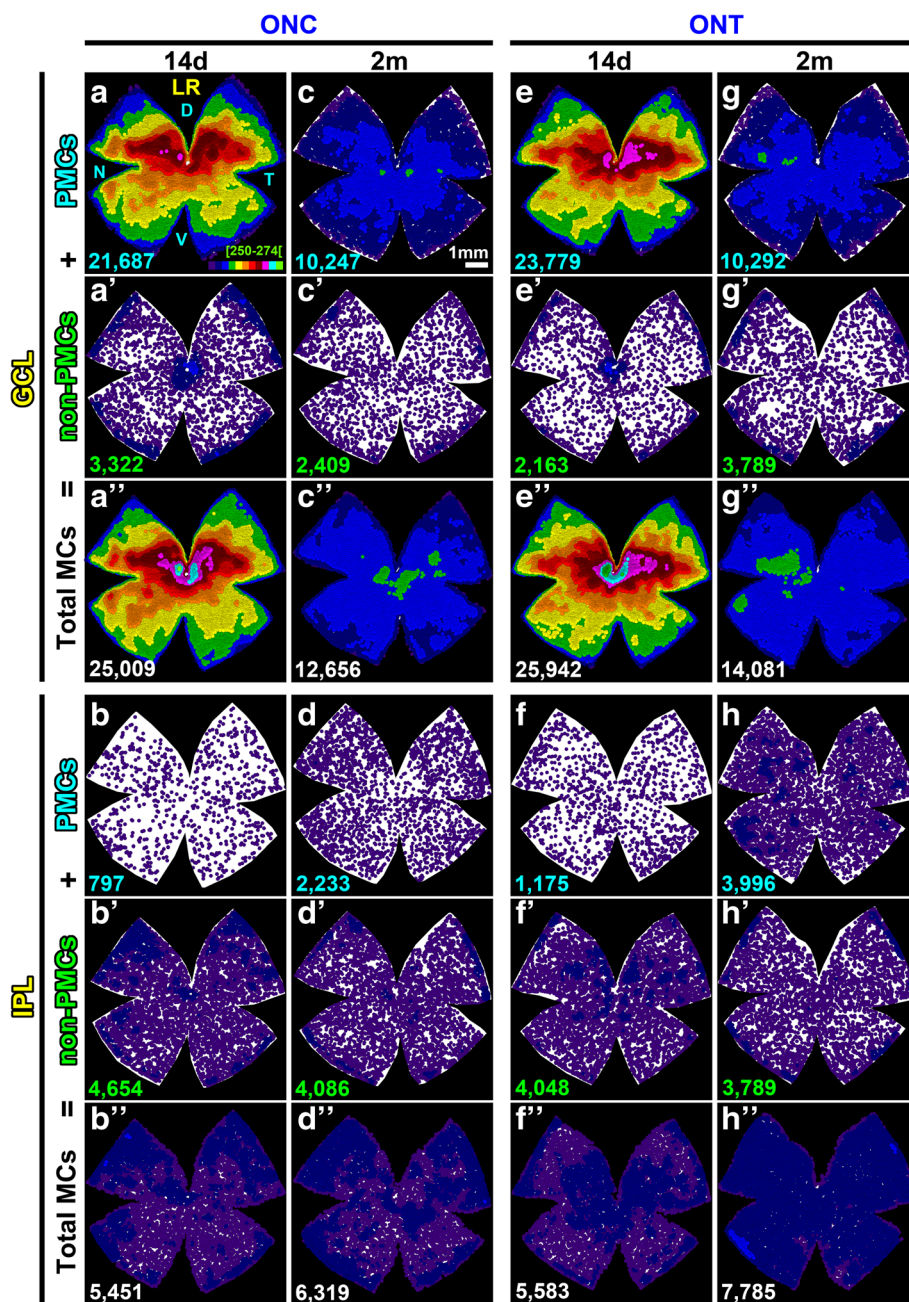


**Fig. 5** Migration of microglial cells between the ganglion cell layer and the inner plexiform layer after axotomy. Neighbor maps showing the spatial distribution of PMCs, non-PMC (non-phagocytic), or total MCs (sum of both) in the ganglion cell complex at 14 days and 2 months post-ONC (a-d) or ONT (e-h). Each column is the same retina, where MCs in the GCL and in the IPL have been analyzed. Map description is in Fig. 1 legend

agreement with other works describing that rod-shaped MCs are induced by the interruption of axonal transport after insults such as axotomy or ocular hypertension [46, 66], but also during aging [67]. Rod-shaped MCs bear the M2 phenotype, and although their function is unknown, it is hypothesized that they protect the degenerating neurons [29, 67, 68]. In apparent contradiction with that hypothesis, we show here that rod-shaped MCs

are or have been involved in the phagocytic response. In other words, either they engulf FG in their rod-shape state, or they could change from an ameboid phagocytic state to a protective rod-shape during the course of RGC degeneration. Because FG is accumulated in the phagolysosomes of MCs for a long time after cleansing the tissue, at least 2 months as shown here, we cannot rule out either possibility.

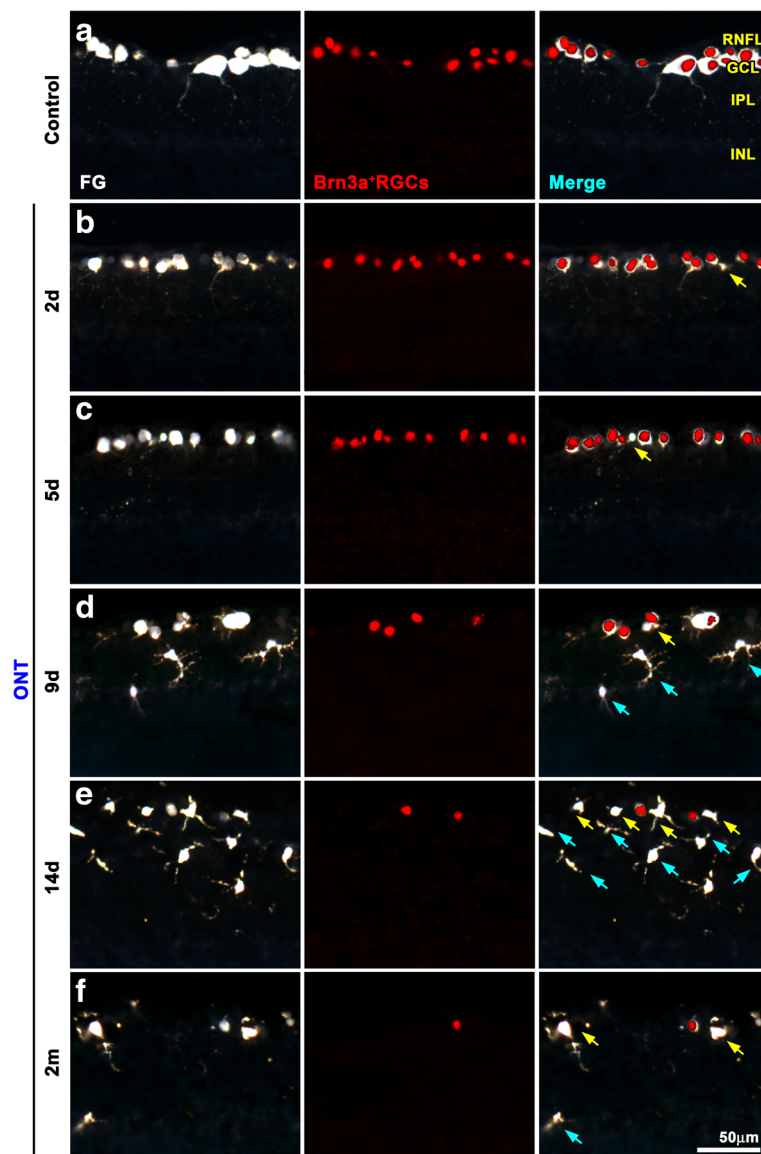


**Fig. 6** PMCs appear first in the ganglion cell layer and afterwards in the inner plexiform layer. Cross sections from control and injured traced retinas immunodetected with Brn3a. **a** Control. **b–f** Injured at increasing times after axotomy. PMCs are observed at 2 and 5 days in the GCL, and they become apparent in the IPL/INL from 9 days onwards. Yellow arrows point to PMCs in the ganglion cell layer and blue ones to PMCs in the plexiform and inner nuclear layers

### RGC death and clearance

One of the most interesting results of this work is the 3 days delay between RGC death and RGC clearance that was observed after both lesions. This means that independently of the course of RGC loss (slower after ONC than after ONT), 3 days are needed for the MCs to become phagocytic. Therefore, to assess RGC death, tracing is not the best approach, particularly when manipulating MCs as neuroprotective tool, because MC inhibition may further delay the removal of dead RGCs from the tissue.

### PMC migration

At 14 days, the number of PMCs in the GCL exceeds the population of SMCs in intact retinas by >10,000. There are several theories to explain this increase: (I) microglial proliferation [69–71], (II) extravasation of monocytes [72], and (III) migration from other retinal layers [59]. With our data, we cannot rule out (I) or (II). We found at 14 days, non-PMCs spread along the GCL, except around the optic nerve and the retinal periphery where they accumulated. They may reflect either local division, or retinal infiltration of monocytes from the

ciliary bodies [73], and the peripapillary region. It is worth noting that these non-PMCs may or may not be activated, and although they have not engulfed RGC somas, they may have phagocytosed RGC axons, which do not accumulate FG. However, we do demonstrate that there is MC migration between the IPL and the GCL that would account for half of the MC surplus. Interestingly, 2 months after either lesion, the number of MCs in the GCL decreases, increasing in the IPL with cells from the GCL as the returning ones are PMCs. Finally, while the number of MCs in the GCL is back to normal, the IPL is short of ~4000 MCs. Have the missing MCs died? Or have they left the retina? We think that the second possibility is more plausible, because MC death would probably cause a second wave of MC activation and phagocytosis.

### Topography

Our state-of-the-art topographical analyses show that more PMCs accumulate in the retinal regions where there is, proportionally, more RGC death. It is important to have in mind that RGC death is diffuse along the retina, meaning that RGCs die synchronously, but more of them die where there are more. Thus, there must be signals from the degenerating neurons and sensors in the MCs that inform of the amount of cell bodies to be removed, and upon them, more or less MCs migrate to the injured zone, having into account that one MC is able to engulf three RGC somas. All in all, these results indicate that phagocytosis is activated by the death of RGCs rather than by the inflicted axonal damage.

Finally, our present data together with a previous work in mice [21] suggest that after optic nerve axotomy, MCs perform a cleansing role, but there is no indication of them being involved in the death of RGCs, at least during the quick phase of loss. In fact, Hilla et al. [74] have recently demonstrated, using an *in vivo* approach to deplete retinal MCs, that these cells do not play an active role on the death of RGCs after optic nerve axotomy.

### Conclusion

In conclusion, after axotomy, RGC death precedes RGC clearance and there is an inverse correlation between RGC loss and PMC appearance, both numerically and topographically. Finally, to cope with the massive axotomy-induced RGC loss, MCs travel from the IPL to the GCL. The system appears restored at 2 months, when the GCL presents a normal number of MCs and the IPL has remodeled to its new status.

### Abbreviations

ARVO: Association for Research in Vision and Ophthalmology; Brn3a: Brain-specific homeobox/POU domain protein 3a; DAPI: 4',6-Diamidino-2-phenylindole; dRGC(s): Displaced retinal ganglion cells; FG: Fluorogold; GCL: Ganglion cell layer; Iba1: Ionized calcium-binding adapter molecule 1; INL: Inner nuclear layer; IPL: Inner plexiform layer; MCs: Microglial cells; n: Sample size; Non-PMC(s): Non-phagocytic microglial cells; OCT: Optimal

cutting temperature; ON: Optic nerve; ONC: Optic nerve crush; ONL: Outer nuclear layer; ONT: Optic nerve transection; OPL: Outer plexiform layer; PMC(s): Phagocytic microglial cells; RGC(s): Retinal ganglion cells; RNFL: Retinal nerve fiber layer; SCi: Superior colliculi; SMC(s): Surveying microglial cells; vs.: Versus

### Acknowledgements

The authors thank Isabel Cánovas-Martínez and Leticia Nieto-Lopez for their technician support. We are thankful to the veterinarians and technicians at the animal housing facilities of the University of Murcia, especially Yolanda Martínez-Verdú and Francisco J. Zapata-Nicolás for their help and support during this long-term experiment.

### Funding

This study was funded by Fundación Séneca, Agencia de Ciencia y Tecnología Región de Murcia (19881/GERM/15), and the Spanish Ministry of Economy and Competitiveness, Instituto de Salud Carlos III, Fondo Europeo de Desarrollo Regional "Una Manera de Hacer Europa" (SAF2015-67643-P, P116/00031).

### Availability of data and materials

Please contact author for data requests.

### Authors' contributions

FMN-N and MA-B conceived and designed the experiments. FMN-N, MS-N, and PS-C performed the experiments. FMN-N did the data collection. MJ-L made the macro-design. FMN-N, MJ-L, MS-N, and MA-B carried out the data analysis. FMN-N and MA-B wrote the manuscript. MA-B and MV-S funded the project. All authors reviewed and approved the final version.

### Ethics approval

All animals were treated in compliance with the European Union guidelines for Animal Care and Use for Scientific Purpose (Directive 2010/63/EU) and the guidelines from the Association for Research in Vision and Ophthalmology (ARVO) Statement for the Use of Animals in Ophthalmic and Vision Research. All procedures were approved by the Ethical and Animal Studies Committee of the University of Murcia, Spain (REGA 300305440012).

### Consent for publication

Not applicable.

### Competing interests

The authors declare that they have no competing interests.

### Publisher's Note

Springer Nature remains neutral with regard to jurisdictional claims in published maps and institutional affiliations.

### Author details

<sup>1</sup>Grupo de Oftalmología Experimental, Instituto Murciano de Investigación Biosanitaria-Virgen de la Arrixaca, Edificio LAIB Planta 5ª, Carretera Buenavista s/n, 30120 El Palmar, Murcia, Spain. <sup>2</sup>Departamento de Oftalmología, Facultad de Medicina, Universidad de Murcia, Murcia, Spain. <sup>3</sup>Present address: Retinal Neurophysiology Section, National Eye Institute, National Institutes of Health, Bethesda, MD 20892, USA.

Received: 31 July 2017 Accepted: 16 October 2017

Published online: 09 November 2017

### References

- Vidal-Sanz M, Galindo-Romero C, Valiente-Soriano FJ, et al. Shared and differential retinal responses against optic nerve injury and ocular hypertension. *Front Neurosci.* 2017;11:235.
- Nadal-Nicolás FM, Sobrado-Calvo P, Jiménez-López M, et al. Long-term effect of optic nerve axotomy on the retinal ganglion cell layer. *Invest Ophthalmol Vis Sci.* 2015;56:6095–112.
- Villegas-Pérez MP, Vidal-Sanz M, Rasminsky M, et al. Rapid and protracted phases of retinal ganglion cell loss follow axotomy in the optic nerve of adult rats. *J Neurobiol.* 1993;24:23–36.
- Sánchez-Migallón MC, Valiente-Soriano FJ, Nadal-Nicolás FM, et al. Apoptotic retinal ganglion cell death after optic nerve transection or crush in mice:

- delayed RGC loss with BDNF or a caspase 3 inhibitor. *Invest Ophthalmol Vis Sci.* 2016;57:81–93.
5. Berkelaar M, Clarke DB, Wang YC, et al. Axotomy results in delayed death and apoptosis of retinal ganglion cells in adult rats. *J Neurosci.* 1994;14:4368–74.
  6. Kerr JF, Wyllie AH, Currie AR. Apoptosis: a basic biological phenomenon with wide-ranging implications in tissue kinetics. *Br J Cancer.* 1972;26:239–57.
  7. Schwartz LM, Smith SW, Jones ME, et al. Do all programmed cell deaths occur via apoptosis? *Proc Natl Acad Sci U S A.* 1993;90:980–4.
  8. Nadal-Nicolás FM, Salinas-Navarro M, Jiménez-López M, et al. Displaced retinal ganglion cells in albino and pigmented rats. *Front Neuroanat.* 2014;6:8:99.
  9. Wang X, Zhao L, Zhang J, et al. Requirement for microglia for the maintenance of synaptic function and integrity in the mature retina. *J Neurosci.* 2016;36:2827–42.
  10. Wong WT. Microglial aging in the healthy CNS: phenotypes, drivers, and rejuvenation. *Front Cell Neurosci.* 2013;13(7):22.
  11. Di Pierdomenico J, García-Ayuso D, Jiménez-López M, et al. Different ipsi- and contralateral glial responses to anti-VEGF and triamcinolone intravitreal injections in rats. *Invest Ophthalmol Vis Sci.* 2016;57:3533–44.
  12. Mac Nair CE, Schlamp CL, Montgomery AD, et al. Retinal glial responses to optic nerve crush are attenuated in Bax-deficient mice and modulated by purinergic signaling pathways. *J Neuroinflammation.* 2016;13:93.
  13. Paques M, Simonutti M, Augustin S, et al. In vivo observation of the locomotion of microglial cells in the retina. *Glia.* 2010;58:1663–8.
  14. Chen L, Yang P, Kijlstra A. Distribution, markers, and functions of retinal microglia. *Ocul Immunol Inflamm.* 2002;10:27–39.
  15. Wolf SA, Boddeke HW, Kettenmann H. Microglia in physiology and disease. *Annu Rev Physiol.* 2017;79:619–43.
  16. Colonna M, Butovsky O. Microglia function in the central nervous system during health and neurodegeneration. *Annu Rev Immunol.* 2017;35:441–68.
  17. Diaz-Aparicio I, Beccari S, Abiega O, Sierra A. Clearing the corpses: regulatory mechanisms, novel tools, and therapeutic potential of harnessing microglial phagocytosis in the diseased brain. *Neural Regen Res.* 2016;11:1533–9.
  18. Zabel MK, Zhao L, Zhang Y, et al. Microglial phagocytosis and activation underlying photoreceptor degeneration is regulated by CX3CL1-CX3CR1 signaling in a mouse model of retinitis pigmentosa. *Glia.* 2016;64:1479–91.
  19. Thanos S. The relationship of microglial cells to dying neurons during natural neuronal cell death and axotomy-induced degeneration of the rat retina. *Eur J Neurosci.* 1991;3:1189–207.
  20. Thanos S, Pavlidis C, Mey J, et al. Specific transcellular staining of microglia in the adult rat after traumatic degeneration of carbocyanine-filled retinal ganglion cells. *Exp Eye Res.* 1992;55:101–17.
  21. Galindo-Romero C, Valiente-Soriano FJ, Jiménez-López M, et al. Effect of brain-derived neurotrophic factor on mouse axotomized retinal ganglion cells and phagocytic microglia. *Invest Ophthalmol Vis Sci.* 2013;54:974–85.
  22. Nadal-Nicolás FM, Jimenez-Lopez M, Salinas-Navarro M, et al. Temporal response of the phagocytic microglia in the axotomized rat retina: optic nerve crush vs. transection. *Acta Ophthalmol.* 2014; 10.1111/j.1755-3768.2014.S007.x.
  23. Vidal-Sanz M, Nadal-Nicolás FM, Sobrado-Calvo P, et al. Quantitative and topographical microglial cell changes in the ganglion cell layer and inner plexiform layer after optic nerve axotomy. *Invest Ophthalmol Vis Sci.* 2016;57:2226.
  24. Nadal-Nicolás FM, Galindo-Romero C, Valiente-Soriano FJ, et al. Involvement of P2X7 receptor in neuronal degeneration triggered by traumatic injury. *Sci Rep.* 2016;6:38499.
  25. Salinas-Navarro M, Mayor-Torroglosa S, Jiménez-López M, et al. A computerized analysis of the entire retinal ganglion cell population and its spatial distribution in adult rats. *Vis Res.* 2009;49:115–26.
  26. Nadal-Nicolás FM, Salinas-Navarro M, Vidal-Sanz M, et al. Two methods to trace retinal ganglion cells with fluorogold: from the intact optic nerve or by stereotactic injection into the optic tract. *Exp Eye Res.* 2015;131:12–9.
  27. Karlstetter M, Scholz R, Rutar M, et al. Retinal microglia: just bystander or target for therapy? *Prog Retin Eye Res.* 2015;45:30–57.
  28. Langmann T. Microglia activation in retinal degeneration. *J Leukoc Biol.* 2007;81:1345–51.
  29. Streit WJ, Walter SA, Pennell NA. Reactive microgliosis. *Prog Neurobiol.* 1999;57:563–81.
  30. Ellis-Behnke RG, Jonas RA, Jonas JB. The microglial system in the eye and brain in response to stimuli in vivo. *J Glaucoma.* 2013;22(Suppl 5):S32–5.
  31. Marín-Teva JL, Cuadros MA, Martín-Oliva D, et al. Microglia and neuronal cell death. *Neuron Glia Biol.* 2011;7:25–40.
  32. Ramirez AI, de Hoz R, Salobar-Garcia E, et al. The role of microglia in retinal neurodegeneration: Alzheimer's disease, Parkinson, and glaucoma. *Front Aging Neurosci.* 2017; 10.3389/fnagi.2017.00214.
  33. Baptista FI, Aveleira CA, Castilho ÁF, et al. Elevated glucose and interleukin-1 $\beta$  differentially affect retinal microglial cell proliferation. *Mediat Inflamm.* 2017; 4316316:2017.
  34. Nadal-Nicolás FM, Jiménez-López M, Sobrado-Calvo P, et al. Brn3a as a marker of retinal ganglion cells: qualitative and quantitative time course studies in naive and optic nerve-injured retinas. *Invest Ophthalmol Vis Sci.* 2009;50:3860–8.
  35. Salinas-Navarro M, Jiménez-López M, Valiente-Soriano FJ, et al. Retinal ganglion cell population in adult albino and pigmented mice: a computerized analysis of the entire population and its spatial distribution. *Vis Res.* 2009;49:637–47.
  36. Parrilla-Reverter G, Agudo M, Nadal-Nicolás F, et al. Time-course of the retinal nerve fibre layer degeneration after complete intra-orbital optic nerve transection or crush: a comparative study. *Vis Res.* 2009;49:2808–25.
  37. Nadal-Nicolás FM, Jiménez-López M, Salinas-Navarro M, et al. Whole number, distribution and co-expression of brn3 transcription factors in retinal ganglion cells of adult albino and pigmented rats. *PLoS One.* 2012; 7(11):e49830.
  38. Nadal-Nicolás FM, Rodríguez-Villagra E, Bravo-Osuna I, et al. Ketorolac administration attenuates retinal ganglion cell death after axonal injury. *Invest Ophthalmol Vis Sci.* 2016;57:1183–92.
  39. Nadal-Nicolás FM, Madeira MH, Salinas-Navarro M, et al. Transient downregulation of melanopsin expression after retrograde tracing or optic nerve injury in adult rats. *Invest Ophthalmol Vis Sci.* 2015;56:4309–23.
  40. Nadal-Nicolás FM, Vidal-Sanz M, Agudo-Barriuso M. The aging rat retina: from function to anatomy. *Neurobiol Aging.* 2017; 10.1016/j.neurobiolaging.2017.09.021.
  41. Gómez-Ramírez AM, Villegas-Pérez MP, Miralles de Imperial J, et al. Effects of intramuscular injection of botulinum toxin and doxorubicin on the survival of abducens motoneurons. *Invest Ophthalmol Vis Sci.* 1999;40:414–24.
  42. Sellés-Navarro I, Villegas-Pérez MP, Salvador-Silva M, et al. Retinal ganglion cell death after different transient periods of pressure-induced ischemia and survival intervals. A quantitative in vivo study. *Invest Ophthalmol Vis Sci.* 1996;37:2002–14.
  43. Ortín-Martínez A, Salinas-Navarro M, Nadal-Nicolás FM, et al. Laser-induced ocular hypertension in adult rats does not affect non-RGC neurons in the ganglion cell layer but results in protracted severe loss of cone-photoreceptors. *Exp Eye Res.* 2015;132:17–33.
  44. Janssen KT, Mac Nair CE, Dietz JA, et al. Nuclear atrophy of retinal ganglion cells precedes the bax-dependent stage of apoptosis. *Invest Ophthalmol Vis Sci.* 2013;54:1805–15.
  45. He T, Mortensen X, Wang P, et al. The effects of immune protein CD3 $\zeta$  development and degeneration of retinal neurons after optic nerve injury. *PLoS One.* 2017;12(4):e0175522.
  46. Sobrado-Calvo P, Vidal-Sanz M, Villegas-Pérez MP. Rat retinal microglial cells under normal conditions, after optic nerve section, and after optic nerve section and intravitreal injection of trophic factors or macrophage inhibitory factor. *J Comp Neurol.* 2007;501(6):866–78.
  47. Cen LP, Han M, Zhou L, et al. Bilateral retinal microglial response to unilateral optic nerve transection in rats. *Neuroscience.* 2015;311:56–66.
  48. García-Valenzuela E, Sharma SC, Piña AL. Multilayered retinal microglial response to optic nerve transection in rats. *Mol Vis.* 2005;11:225–31.
  49. Santos AM, Calvente R, Tassi M, et al. Embryonic and postnatal development of microglial cells in the mouse retina. *J Comp Neurol.* 2008;506:224–39.
  50. Lee JE, Liang KJ, Fariss RN, et al. Ex vivo dynamic imaging of retinal microglia using time-lapse confocal microscopy. *Invest Ophthalmol Vis Sci.* 2008;49:4169–76.
  51. Bodeutsch N, Siebert H, Dermon C, et al. Unilateral injury to the adult rat optic nerve causes multiple cellular responses in the contralateral site. *J Neurobiol.* 1999;38:116–28.
  52. Ito D, Imai Y, Ohsawa K, et al. Microglia-specific localisation of a novel calcium binding protein, Iba1. *Brain Res Mol Brain Res.* 1998;57:1–9.
  53. Panagis L, Thanos S, Fischer D, et al. Unilateral optic nerve crush induces bilateral retinal glial cell proliferation. *Eur J Neurosci.* 2005;21:2305–9.
  54. Liu S, Li ZW, Weinreb RN, et al. Tracking retinal microgliosis in models of retinal ganglion cell damage. *Invest Ophthalmol Vis Sci.* 2012;53:6254–62.

55. Ramírez AI, Salazar JJ, de Hoz R, et al. Quantification of the effect of different levels of IOP in the astroglia of the rat retina ipsilateral and contralateral to experimental glaucoma. *Invest Ophthalmol Vis Sci*. 2010;51:5690–6.
56. Müller M, Holländer H. A small population of retinal ganglion cells projecting to the retina of the other eye. An experimental study in the rat and the rabbit. *Exp Brain Res*. 1988;71:611–7.
57. Avellaneda-Chevrier VK, Wang X, Hooper ML, et al. The retino-retinal projection: tracing retinal ganglion cells projecting to the contralateral retina. *Neurosci Lett*. 2015;591:105–9.
58. Nadal-Nicolás FM, Valiente-Soriano FJ, Salinas-Navarro M, et al. Retino-retinal projection in juvenile and young adult rats and mice. *Exp Eye Res*. 2015;134:47–52.
59. Thanos S, Richter W. The migratory potential of vitally labelled microglial cells within the retina of rats with hereditary photoreceptor dystrophy. *Int J Dev Neurosci*. 1993;11:671–80.
60. Madeira MH, Boia R, Santos PF, et al. Contribution of microglia-mediated neuroinflammation to retinal degenerative diseases. *Mediat Inflamm*. 2015;673090:2015.
61. Chen Z, Jalabi W, Shpargel KB, et al. Lipopolysaccharide-induced microglial activation and neuroprotection against experimental brain injury is independent of hematogenous TLR4. *J Neurosci*. 2012;32:11706–15.
62. Karlstetter M, Ebert S, Langmann T. Microglia in the healthy and degenerating retina: insights from novel mouse models. *Immunobiology*. 2010;215:685–91.
63. Madeira MH, Elvas F, Boia R, et al. Adenosine A2AR blockade prevents neuroinflammation-induced death of retinal ganglion cells caused by elevated pressure. *J Neuroinflammation*. 2015;12:115.
64. Davis BM, Salinas-Navarro M, Cordeiro MF, et al. Characterizing microglia activation: a spatial statistics approach to maximize information extraction. *Sci Rep*. 2017;7:1576.
65. Jonas RA, Yuan TF, Liang YX, et al. The spider effect: morphological and orienting classification of microglia in response to stimuli in vivo. *PLoS One*. 2012;7(2):e30763.
66. de Hoz R, Gallego BI, Ramírez AI, et al. Rod-like microglia are restricted to eyes with laser-induced ocular hypertension but absent from the microglial changes in the contralateral untreated eye. *PLoS One*. 2013;8(12):e83733.
67. Bachstetter AD, Ighodaro ET, Hassoun Y, et al. Rod-shaped microglia morphology is associated with aging in 2 human autopsy series. *Neurobiol Aging*. 2017;52:98–105.
68. Trapp BD, Wujek JR, Criste GA, et al. Evidence for synaptic stripping by cortical microglia. *Glia*. 2007;55:360–8.
69. Garcia-Valenzuela E, Sharma SC. Laminar restriction of retinal macrophagic response to optic nerve axotomy in the rat. *J Neurobiol*. 1999;40:55–66.
70. Wohl SG, Schmeer CW, Witte OW, et al. Proliferative response of microglia and macrophages in the adult mouse eye after optic nerve lesion. *Invest Ophthalmol Vis Sci*. 2010;51:2686–96.
71. Wohl SG, Schmeer CW, Frieze T, et al. In situ dividing and phagocytosing retinal microglia express nestin, vimentin, and NG2 in vivo. *PLoS One*. 2011; 6(8):e22408.
72. Trost A, Motloch K, Bruckner D, et al. Time-dependent retinal ganglion cell loss, microglial activation and blood-retina-barrier tightness in an acute model of ocular hypertension. *Exp Eye Res*. 2015;136:59–71.
73. Zhang Y, Zhao L, Wang X, et al. Microglia homeostasis in the adult mouse retina: restoration of microglial distribution, morphology, and function following acute depletion. *Invest Ophthalmol Vis Sci*. 2017;58:806.
74. Hilla AM, Diekmann H, Fischer D. Microglia are irrelevant for neuronal degeneration and axon regeneration after acute injury. *J Neurosci*. 2017;37: 6113–24.

Submit your next manuscript to BioMed Central and we will help you at every step:

- We accept pre-submission inquiries
- Our selector tool helps you to find the most relevant journal
- We provide round the clock customer support
- Convenient online submission
- Thorough peer review
- Inclusion in PubMed and all major indexing services
- Maximum visibility for your research

Submit your manuscript at  
[www.biomedcentral.com/submit](http://www.biomedcentral.com/submit)

